



CERN-EP-2016-???
September 26, 2016

Azimuthal asymmetries of charged hadrons produced in high-energy muon scattering off longitudinally polarised deuterons

The COMPASS Collaboration

Abstract

Single hadron azimuthal asymmetries in the cross sections of positive and negative hadron production in muon semi-inclusive deep inelastic scattering off longitudinally polarised deuterons are determined using the 2006 COMPASS data and also all deuteron COMPASS data. For each hadron charge, the dependence of the azimuthal asymmetry on the hadron azimuthal angle ϕ is obtained by means of a five-parameter fitting function that besides a ϕ -independent term includes four modulations predicted by theory: $\sin \phi$, $\sin 2\phi$, $\sin 3\phi$ and $\cos \phi$. The amplitudes of the five terms have been first extracted for the data integrated over all kinematic variables. In further fits, the ϕ -dependence is determined as a function of one of three kinematic variables (Bjorken- x , fractional energy of virtual photon taken by the outgoing hadron and hadron transverse momentum), while disregarding the other two. Except the ϕ -independent term, all the modulation amplitudes are very small, and no clear kinematic dependence could be observed within experimental uncertainties.

PACS: 13.60.Hb, 13.85.Hd, 13.85.Ni, 13.88.+e

Keywords: lepton deep inelastic scattering, polarisation, spin asymmetry, parton distribution functions

(To be submitted to the European Physical Journal C)

The COMPASS Collaboration

C. Adolph⁹, M. Aghasyan²⁶, R. Akhunzyanov⁸, M.G. Alexeev²⁸, G.D. Alexeev⁸, A. Amoroso^{28,29}, V. Andrieux^{30,22}, N.V. Anfimov⁸, V. Anosov⁸, K. Augsten^{8,20}, W. Augustyniak³¹, A. Austregesilo¹⁷, C.D.R. Azevedo², B. Badełek³², F. Balestra^{28,29}, M. Ball⁴, J. Barth⁵, R. Beck⁴, Y. Bedfer²², J. Bernhard^{14,11}, K. Bicker^{17,11}, E. R. Bielert¹¹, R. Birsa²⁶, M. Bodlak¹⁹, P. Bordalo^{13,a}, F. Bradamante^{25,26}, C. Braun⁹, A. Bressan^{25,26}, M. Büchele¹⁰, W.-C. Chang²³, C. Chatterjee⁷, M. Chiosso^{28,29}, I. Choi³⁰, S.-U. Chung^{17,b}, A. Cicuttin^{27,26}, M.L. Crespo^{27,26}, Q. Curiel²², S. Dalla Torre²⁶, S.S. Dasgupta⁷, S. Dasgupta^{25,26}, O.Yu. Denisov^{29,#}, L. Dhara⁷, S.V. Donskov²¹, N. Doshita³⁴, Ch. Dreisbach¹⁷, V. Duic²⁵, W. Dünnweber^c, M. Dziewiecki³³, A. Efremov^{8,#}, P.D. Eversheim⁴, W. Eyrich⁹, M. Faessler^c, A. Ferrero²², M. Finger¹⁹, M. Finger jr.¹⁹, H. Fischer¹⁰, C. Franco¹³, N. du Fresne von Hohenesche¹⁴, J.M. Friedrich¹⁷, V. Frolov^{8,11}, E. Fuchey²², F. Gautheron³, O.P. Gavrichtchouk⁸, S. Gerassimov^{16,17}, J. Giarra¹⁴, F. Giordano³⁰, I. Gnesi^{28,29}, M. Gorzellik^{10,1}, S. Grabmüller¹⁷, A. Grasso^{28,29}, M. Grosse Perdekamp³⁰, B. Grube¹⁷, T. Grussenmeyer¹⁰, A. Guskov⁸, F. Haas¹⁷, D. Hahne⁵, G. Hamar^{25,26}, D. von Harrach¹⁴, F.H. Heinsius¹⁰, R. Heitz³⁰, F. Herrmann¹⁰, N. Horikawa^{18,d}, N. d'Hose²², C.-Y. Hsieh^{23,e}, S. Huber¹⁷, S. Ishimoto^{34,f}, A. Ivanov^{28,29}, Yu. Ivanshin⁸, T. Iwata³⁴, V. Jary²⁰, R. Joosten⁴, P. Jörg¹⁰, E. Kabuß¹⁴, B. Ketzer⁴, G.V. Khaustov²¹, Yu.A. Khokhlov^{21,g,h}, Yu. Kisselev⁸, F. Klein⁵, K. Klimaszewski³¹, J.H. Koivuniemi³, V.N. Kolosov²¹, K. Kondo³⁴, K. Königsmann¹⁰, I. Konorov^{16,17}, V.F. Konstantinov²¹, A.M. Kotzinian^{28,29}, O.M. Kouznetsov⁸, M. Krämer¹⁷, P. Kremser¹⁰, F. Krinner¹⁷, Z.V. Kroumchtein⁸, Y. Kulinich³⁰, F. Kunne²², K. Kurek³¹, R.P. Kurjata³³, A.A. Lednev^{21,*}, A. Lehmann⁹, M. Levillain²², S. Levorato²⁶, Y.-S. Lian^{23,j}, J. Lichtenstadt²⁴, R. Longo^{28,29}, A. Maggiora²⁹, A. Magnon³⁰, N. Makins³⁰, N. Makke^{25,26}, G.K. Mallot^{11,#}, B. Marianski³¹, A. Martin^{25,26}, J. Marzec³³, J. Matoušek^{19,26}, H. Matsuda³⁴, T. Matsuda¹⁵, G.V. Meshcheryakov⁸, M. Meyer^{30,22}, W. Meyer³, Yu.V. Mikhailov²¹, M. Mikhasenko⁴, E. Mitrofanov⁸, N. Mitrofanov⁸, Y. Miyachi³⁴, A. Nagaytsev⁸, F. Nerling¹⁴, D. Neyret²², J. Nový^{20,11}, W.-D. Nowak¹⁴, G. Nukazuka³⁴, A.S. Nunes¹³, A.G. Olshevsky⁸, I. Orlov⁸, M. Ostrick¹⁴, D. Panzieri^{1,29}, B. Parsamyan^{28,29}, S. Paul¹⁷, J.-C. Peng³⁰, F. Pereira², M. Pešek¹⁹, D.V. Peshekhonov⁸, N. Pierre^{14,22}, S. Platchkov²², J. Pochodzalla¹⁴, V.A. Polyakov²¹, J. Pretz^{5,i}, M. Quaresma¹³, C. Quintans¹³, S. Ramos^{13,a}, C. Regali¹⁰, G. Reicherz³, C. Riedl³⁰, M. Roskot¹⁹, N.S. Rossiyskaya⁸, D.I. Ryabchikov^{21,h}, A. Rybnikov⁸, A. Rychter³³, R. Salac²⁰, V.D. Samoilenko²¹, A. Sandacz³¹, C. Santos²⁶, S. Sarkar⁷, I.A. Savin⁸, T. Sawada²³, G. Sbrizzai^{25,26}, P. Schiavon^{25,26}, K. Schmidt^{10,1}, H. Schmieden⁵, K. Schönning^{11,k}, E. Seder²², A. Selyunin⁸, L. Silva¹³, L. Sinha⁷, S. Sirtl¹⁰, M. Slunecka⁸, J. Smolik⁸, A. Srnka⁶, D. Steffen^{11,17}, M. Stolarski¹³, O. Subrt^{11,20}, M. Sulc¹², H. Suzuki^{34,d}, A. Szabelski^{31,26}, T. Szameitat^{10,1}, P. Sznajder³¹, S. Takekawa^{28,29}, M. Tasevsky⁸, S. Tessaro²⁶, F. Tessarotto²⁶, F. Thibaud²², A. Thiel⁴, F. Tosello²⁹, V. Tskhay¹⁶, S. Uhl¹⁷, J. Veloso², M. Virius²⁰, J. Vondra²⁰, S. Wallner¹⁷, T. Weisrock¹⁴, M. Wilfert¹⁴, J. ter Wolbeek^{10,1}, K. Zaremba³³, P. Zavada⁸, M. Zavertyaev¹⁶, E. Zemlyanichkina⁸, N. Zhuravlev⁸, M. Ziembicki³³ and A. Zink⁹

¹ University of Eastern Piedmont, 15100 Alessandria, Italy

² University of Aveiro, Department of Physics, 3810-193 Aveiro, Portugal

³ Universität Bochum, Institut für Experimentalphysik, 44780 Bochum, Germany^{mn}

⁴ Universität Bonn, Helmholtz-Institut für Strahlen- und Kernphysik, 53115 Bonn, Germany^m

⁵ Universität Bonn, Physikalisches Institut, 53115 Bonn, Germany^m

⁶ Institute of Scientific Instruments, AS CR, 61264 Brno, Czech Republic^o

⁷ Matrivani Institute of Experimental Research & Education, Calcutta-700 030, India^p

⁸ Joint Institute for Nuclear Research, 141980 Dubna, Moscow region, Russia^q

⁹ Universität Erlangen–Nürnberg, Physikalisches Institut, 91054 Erlangen, Germany^m

¹⁰ Universität Freiburg, Physikalisches Institut, 79104 Freiburg, Germany^{mn}

¹¹ CERN, 1211 Geneva 23, Switzerland

¹² Technical University in Liberec, 46117 Liberec, Czech Republic^o

- ¹³ LIP, 1000-149 Lisbon, Portugal^f
- ¹⁴ Universität Mainz, Institut für Kernphysik, 55099 Mainz, Germany^m
- ¹⁵ University of Miyazaki, Miyazaki 889-2192, Japan^s
- ¹⁶ Lebedev Physical Institute, 119991 Moscow, Russia
- ¹⁷ Technische Universität München, Physik Department, 85748 Garching, Germany^{mc}
- ¹⁸ Nagoya University, 464 Nagoya, Japan^s
- ¹⁹ Charles University in Prague, Faculty of Mathematics and Physics, 18000 Prague, Czech Republic^o
- ²⁰ Czech Technical University in Prague, 16636 Prague, Czech Republic^o
- ²¹ State Scientific Center Institute for High Energy Physics of National Research Center ‘Kurchatov Institute’, 142281 Protvino, Russia
- ²² IRFU, CEA, Université Paris-Saclay, 91191 Gif-sur-Yvette, Franceⁿ
- ²³ Academia Sinica, Institute of Physics, Taipei 11529, Taiwan
- ²⁴ Tel Aviv University, School of Physics and Astronomy, 69978 Tel Aviv, Israel^l
- ²⁵ University of Trieste, Department of Physics, 34127 Trieste, Italy
- ²⁶ Trieste Section of INFN, 34127 Trieste, Italy
- ²⁷ Abdus Salam ICTP, 34151 Trieste, Italy
- ²⁸ University of Turin, Department of Physics, 10125 Turin, Italy
- ²⁹ Torino Section of INFN, 10125 Turin, Italy
- ³⁰ University of Illinois at Urbana-Champaign, Department of Physics, Urbana, IL 61801-3080, USA
- ³¹ National Centre for Nuclear Research, 00-681 Warsaw, Poland^u
- ³² University of Warsaw, Faculty of Physics, 02-093 Warsaw, Poland^u
- ³³ Warsaw University of Technology, Institute of Radioelectronics, 00-665 Warsaw, Poland^u
- ³⁴ Yamagata University, Yamagata 992-8510, Japan^s
- * Deceased
- # Corresponding authors
- ^a Also at Instituto Superior Técnico, Universidade de Lisboa, Lisbon, Portugal
- ^b Also at Department of Physics, Pusan National University, Busan 609-735, Republic of Korea and at Physics Department, Brookhaven National Laboratory, Upton, NY 11973, USA
- ^c Supported by the DFG cluster of excellence ‘Origin and Structure of the Universe’ (www.universe-cluster.de)
- ^d Also at Chubu University, Kasugai, Aichi 487-8501, Japan^s
- ^e Also at Department of Physics, National Central University, 300 Jhongda Road, Jhongli 32001, Taiwan
- ^f Also at KEK, 1-1 Oho, Tsukuba, Ibaraki 305-0801, Japan
- ^g Also at Moscow Institute of Physics and Technology, Moscow Region, 141700, Russia
- ^h Supported by Presidential grant NSH-999.2014.2
- ⁱ Present address: RWTH Aachen University, III. Physikalisches Institut, 52056 Aachen, Germany
- ^j Also at Department of Physics, National Kaohsiung Normal University, Kaohsiung County 824, Taiwan
- ^k Present address: Uppsala University, Box 516, 75120 Uppsala, Sweden
- ^l Supported by the DFG Research Training Group Programmes 1102 and 2044
- ^m Supported by the German Bundesministerium für Bildung und Forschung
- ⁿ Supported by EU FP7 (HadronPhysics3, Grant Agreement number 283286)
- ^o Supported by Czech Republic MEYS Grant LG13031
- ^p Supported by SAIL (CSR), Govt. of India
- ^q Supported by CERN-RFBR Grant 12-02-91500
- ^r Supported by the Portuguese FCT - Fundação para a Ciência e Tecnologia, COMPETE and QREN, Grants CERN/FP 109323/2009, 116376/2010, 123600/2011 and CERN/FIS-NUC/0017/2015
- ^s Supported by the MEXT and the JSPS under the Grants No.18002006, No.20540299 and No.18540281; Daiko Foundation and Yamada Foundation

^t Supported by the Israel Academy of Sciences and Humanities

^u Supported by the Polish NCN Grant 2015/18/M/ST2/00550

1 Introduction

Measurements of Semi-Inclusive Deep-Inelastic Scattering (SIDIS)

$$\mu + N \rightarrow \mu' + nh + X, \quad n = 1, 2, \dots \quad (1)$$

of high-energy polarised muons μ off polarised nucleons N in the initial state and scattered muons μ' , $n = 1, 2, \dots$ hadrons h and unobserved particles X in the final state are sensitive to the spin-dependent Parton Distribution Functions (PDFs) of nucleons. The SIDIS cross section depends, in particular, on the azimuthal angle of the produced hadron (see e.g. Ref. [1]), which leads to azimuthal asymmetries related to convolutions of the nucleon Transverse-Momentum-Dependent (TMD) PDFs and parton-to-hadron Fragmentation Functions (FFs).

The TMD PDFs were studied in a number of experiments. The most complete data were obtained by the COMPASS Collaboration at CERN using unpolarised [2], longitudinally and transversely polarised ${}^6\text{LiD}$ (“deuteron”) [3] and NH_3 (“proton”) targets [4]. The data on hadron production off longitudinally polarised deuterons were collected in 2002, 2003, 2004 and 2006 and those off protons in 2007 and 2011. The results on azimuthal asymmetries in charged hadron production off longitudinally polarised deuterons based on the data taken in 2002–2004 were published in Ref. [5]. In 2006 the data were taken with a modified set-up (see e.g. Ref. [6]). The results of the analysis of these data are presented in this Paper as well as those of the combined 2002–2006 data. The analysis of the proton data is in progress.

The Paper is organised as follows. The SIDIS kinematics, basic formulae and a brief theoretical overview are given in Section 2. The analysis of the 2006 data is described in Section 3. The results of the analysis of the combined 2002–2006 data are presented in Section 4. Systematic uncertainties are discussed in Section 5 and conclusions are given in Section 6.

2 Theoretical framework

The SIDIS kinematics are illustrated in Fig. 1(a). The 4-momenta of the incident and scattered muons are denoted by l and l' , respectively. The 4-momentum of the virtual photon is given by $q = l - l'$ with $Q^2 = -q^2$. The angle of the momentum vector \mathbf{q} of the virtual photon with respect to the incident muon in the laboratory frame is denoted by θ_γ . The vectors \mathbf{p}^h and \mathbf{P}_\parallel denote the hadron momentum and the longitudinal target deuteron polarisation, respectively. Their transverse components \mathbf{p}_T^h and \mathbf{P}_T are defined with respect to the virtual-photon momentum. The longitudinal component $|\mathbf{P}_L| = |\mathbf{P}_\parallel| \cos \theta_\gamma$ is approximately equal to $|\mathbf{P}_\parallel|$ due to the smallness of the angle θ_γ . The small transverse component is equal to $|\mathbf{P}_T| = |\mathbf{P}_\parallel| \sin \theta_\gamma$, where $\sin \theta_\gamma \approx 2(Mx/Q)\sqrt{1-y}$, M is the nucleon mass and $y = (qp)/(pl)$ is the fractional energy of the virtual photon, where p is the 4-momentum of the target nucleon. The angle ϕ denotes the azimuthal angle between the lepton scattering plane and the hadron production plane, and ϕ_S is the angle of the target spin with respect to the scattering plane: $\phi_S = 0$ or π for target spin parallel

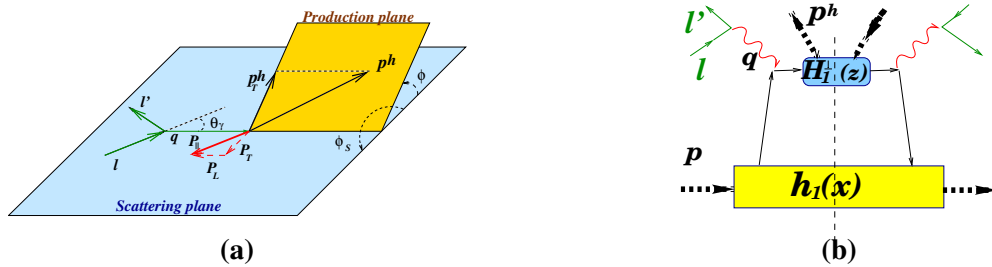


Fig. 1: (a) The SIDIS kinematics shown for target deuteron polarisation \mathbf{P}_\parallel antiparallel to the beam direction. (b) The diagram describing the contribution to the SIDIS cross section of PDF $h_1(x)$ convoluted with the Collins FF $H_1^\perp(z)$.

or antiparallel to the beam direction. Furthermore, we define the Bjorken variable $x_{Bj} \equiv x = Q^2/(2pq)$, the fraction of the virtual-photon energy taken by a hadron, $z = (pp^h)/(pq)$, and the invariant mass of the photon-nucleon system, $W^2 = (p+q)^2$ that at $Q^2 > 1$ (GeV/c)² and $0 < y < 1$ characterise SIDIS.

The general expression for the differential SIDIS cross section (see Ref. [1]) is a linear function of the incident muon polarisation P_μ and of the longitudinal and transverse components \mathbf{P}_L and \mathbf{P}_T of the target deuteron polarisation \mathbf{P}_\parallel :

$$d\sigma = d\sigma_{00} + P_\mu d\sigma_{L0} + \mathbf{P}_L (d\sigma_{0L} + P_\mu d\sigma_{LL}) + \mathbf{P}_T (d\sigma_{0T} + P_\mu d\sigma_{LT}). \quad (2)$$

Here, the first (second) subscript of the partial cross section refers to the beam (target) polarisation: 0, L or T denote unpolarised, longitudinally or transversely polarised.

The azimuthal asymmetries of charged hadron production $a_{h^\pm}(\phi)$ are defined as follows:

$$a_{h^\pm}(\phi) \equiv \frac{d\sigma^{\leftarrow\Rightarrow} - d\sigma^{\leftarrow\leftarrow}}{|P_L|(d\sigma^{\leftarrow\Rightarrow} + d\sigma^{\leftarrow\leftarrow})} = -\frac{d\sigma_{0L} + P_\mu d\sigma_{LL} - \tan\theta_\gamma (d\sigma_{0T} + P_\mu d\sigma_{LT})}{d\sigma_{00} + P_\mu d\sigma_{L0}}, \quad (3)$$

where all cross sections are functions of the angle ϕ . The left part of Eq. (3) represents the experimentally measured asymmetries, which are expected to be positive [3, 5], while the right part shows the expected contributions from the partial cross sections of Eq. (2). The first (second) superscript in the left part of Eq. (3) denotes the beam (target) spin orientation. The symbol \leftarrow denotes the incident muon spin orientation that in the case of a positive charge of the incident muons is mainly opposite to the beam direction. The average value of P_μ is equal to -0.8 . The symbol \Rightarrow or \leftarrow denotes the target deuteron spin orientation (polarisation) being parallel (+) or opposite (−) to the beam direction. The leading term in the right part of Eq. (3) is $d\sigma_{LL}$. To be positive, the right part of Eq. (3) must have the general minus sign in front of it. The contributions of the partial cross sections $d\sigma_{0T}$ and $d\sigma_{LT}$ are suppressed by the small value of $\tan\theta_\gamma = |\mathbf{P}_T|/|\mathbf{P}_L|$.

Following phenomenological considerations based on the QCD parton model of the nucleon and SIDIS in one-photon exchange approximation (see e.g. references in Ref. [5]), the squared modulus of the matrix element defining the cross sections is represented by a number of diagrams. As an example,¹ the diagram accounting for the contribution to the SIDIS cross section of the chiral-odd transversity PDF $h_1(x)$ convoluted with the chiral-odd Collins FF $H_1^\perp(z)$ is shown in Fig. 1(b). The diagram contributes to the asymmetry Eq. (3) via the term $d\sigma_{0T}$. Possible contributions of other PDFs to the cross sections of spinless or unpolarised hadron production off longitudinally polarised deuterons and their expected azimuthal modulations are given in Ref. [5], where only the terms up to the order of M/Q are retained:

$$a_{h^\pm}(\phi) = a_{h^\pm}^0 + a_{h^\pm}^{\sin\phi} \sin\phi + a_{h^\pm}^{\sin 2\phi} \sin 2\phi + a_{h^\pm}^{\sin 3\phi} \sin 3\phi + a_{h^\pm}^{\cos\phi} \cos\phi. \quad (4)$$

Except of the terms with amplitudes $a_{h^\pm}^0$ and $a_{h^\pm}^{\sin 2\phi}$, which are related to the twist-2 helicity PDF g_{1L} and the worm-gear-L PDF h_{1L}^\perp , respectively, none of the modulations were unambiguously observed so far for longitudinally polarised deuterons [7]. The other amplitudes in Eq. (4) are either related to twist-3 PDFs or to twist-2 PDFs suppressed by the small factor $\tan\theta_\gamma$, i.e. transversity PDF h_1 and Sivers PDF f_{1T}^\perp in $a_{h^\pm}^{\sin\phi}$, pretzelosity PDF h_{1T}^\perp in $a_{h^\pm}^{\sin 3\phi}$ and worm-gear-T PDF g_{1T} in $a_{h^\pm}^{\cos\phi}$. The COMPASS results [5] obtained from the 2002–2004 data showed some indications for a possible x -dependence of the modulation amplitudes $a_{h^\pm}^{\sin 2\phi}$ and $a_{h^\pm}^{\cos\phi}$. In Equation (4) we disregarded the contribution of the term with amplitude $a^{\cos 2\phi}$, which could have appeared from $d\sigma_{00}$ in the denominator of Eq. (3). This amplitude is expected [2, 8, 9] to be of the order of 0.1 and would enter Eq. (4) with the factor $a_{h^\pm}^0$ that is of the order of 10^{-3} (see Table 2). This is beyond our experimental accuracy. The same comments apply to possible contributions of terms with amplitudes $a^{\cos\phi}$ and $a^{\sin\phi}$ which also originate from the denominator of

¹In this paper we follow the Amsterdam notations for PDFs and PFFs, see e.g. Ref. [1].

Eq. (3). The small impact of the disregarded modulations on the amplitudes in Eq. (4) is confirmed by the 2006 data (see Section 3.7).

The aim of this study is to continue searches for possible modulations in $a_{h^\pm}(\phi)$ as manifestation of TMD PDFs describing the nucleons in the deuteron and to investigate the x , z and p_T^h dependences of the corresponding modulation amplitudes. For these purposes, we use the 2006 deuteron data and then the combination of all COMPASS deuteron data with longitudinal target polarisation.

3 The 2006 data analysis

3.1 Experimental set-up

The COMPASS set-up is a two-stage forward spectrometer with the world's largest polarised target, two large-aperture magnets SM1 and SM2, various types of tracking and particle identification detectors (PID). The spectrometer was operated in the high energy (160 GeV) muon beam at CERN. Its initial configuration, used for data taking in 2002–2004, was described in Ref. [10]. During the long accelerator shutdown in 2005, the set-up was modified as described in Ref. [6]. The major modifications influencing the present analysis were as follows: (i) the replacement of the two 60 cm long target cells (denoted as U and D) by three cells U , M and D of lengths 30 cm, 60 cm and 30 cm, (ii) the replacement of the target solenoid magnet by the new one with a wider aperture and (iii) the installation of the electromagnetic calorimeter ECAL1 in front of the hadron calorimeter HCAL1. These modifications of the apparatus aimed at further minimising systematic uncertainties, increasing the acceptance of the spectrometer and improving its e/γ PID capabilities.

In 2006, data were taken in two groups of periods. Each group is characterised by its initial set of polarisations in the target cells, which are obtained by using different frequencies of the microwave field to polarise the target material in different cells. We denote one group by G1 and the other one by G2. Each period includes a certain number of intervals of continuous data taking (referred to as runs). The G1 data taking periods started with the initial setting of positive deuteron polarisation in target cells U and D and the negative one in cell M , both corresponding to the positive direction, $f = +$ (along the beam direction), of the solenoid field holding the polarisations. After taking some number of runs, the field was reversed to $f = -$ causing the reversal of the target cell polarisations, so that the data were taken with opposite deuteron polarisations in the cells. The periodic reversal of polarisations continued up to the end of G1 periods. Within the periods, the cell polarisations needed for asymmetries calculation (see Section 3.6) were measured for each run in order to make sure that they are stable and at the level of about 55%. If polarisations dropped below this limit, they were restored by the microwave field before the beginning of the next period. For G2 periods, the procedure was analogous but the initial setting of polarisation in the cells was opposite to the one in G1 at the same field $f = +$. The periodic reversal of the cell polarisations within each group of periods was used to estimate a possible time-dependent systematics of the data. The change of the initial setting of the cell polarisations was used to estimate a possible systematic change of the spectrometer acceptance due to superposition of the target field and the field of SM1. If there is no such systematic change, the acceptance in G1 and G2 periods must be the same for stable performance of the spectrometer.

3.2 Selection of SIDIS events and hadrons

The overall statistics of 2006 comprise about 44.6×10^6 preselected candidates for inclusive DIS (i.e. without hadrons in Eq. (1)) and SIDIS events with $Q^2 > 1$ (GeV/c)². The sample was obtained after rejection of runs that did not pass the data stability tests (see Section 3.3) and events that did not pass the reconstruction tests. The latter were rejected if the z -coordinate of the interaction point (vertex) was determined with an uncertainty larger than 3σ of average.

The selection of SIDIS events from the preselected sample was done as described in Ref. [5]. For each

SIDIS event, a reconstructed vertex with incoming and outgoing muons and one or more additional tracks were required. Trajectories of the incoming muons were required to traverse all target cells. The cuts were applied on the quality of the reconstructed tracks from vertices, the effective lengths of the target cells (28 cm, 56 cm, 28 cm), the momentum of incoming muons (140 GeV/c–180 GeV/c), the fractional energy carried by all tracks from the event ($z < 1$) and the fractional virtual-photon energy ($0.1 < y < 0.9$). About 36.6×10^6 SIDIS events remained for further analysis after cuts.

The tracks from SIDIS events were identified as hadrons using the information from the hadron calorimeters HCAL1 or HCAL2. The distribution of track multiplicity in the SIDIS events peaks at four. A track was identified as a hadron, if its transverse momentum was larger than 0.05 GeV/c, if it is produced in the current fragmentation region as defined by the c.m. Feynman variable $x_F \approx z - (E_T^h)^2 / (zW^2) > 0$, and if it was associated with a cluster in one of the hadron calorimeters with an energy deposit greater than 5 GeV in HCAL1 or greater than 7 GeV in HCAL2. All hadrons in each SIDIS event were included into the analysis of asymmetries. The total number of hadrons in the data of 2006 after all cuts was 15.6×10^6 compared to 53×10^6 in 2002–2004. The number of hadrons in 2006, compared to expectations based on the statistics of 2002–2004, was smaller by a factor of about two because ECAL1 was not fully operational in 2006 yet and partially worked as a hadron absorber in front of HCAL1.

3.3 Tests of data stability

Taking advantage of the three-cell polarised target, stability tests for the 2006 data were performed by investigating variations from run to run for certain observables via ratios R_i , where i is the run number, using the combined information from cells U and D denoted by $(U + D)$, and that of cell M . One expects the ratio $R_i = (U_i + D_i) / M_i$ to be independent of luminosity, close to unity and stable from run to run. In order to confirm this expectation, the ratios R_i per run were obtained for the following observables that are relevant to the selection of SIDIS events and hadrons: number of SIDIS events, number of tracks per SIDIS event, number of clusters in HCAL1 (HCAL2) with $E > 5$ (7) GeV, number of clusters associated with tracks in HCAL1 (HCAL2), average energy of clusters per event in HCAL1 (HCAL2), average energy of the associated clusters per event in HCAL1 (HCAL2) and average angle $\langle \phi \rangle$ between muon scattering and hadron production planes. The R_i values as a function of the run number were fitted by constants \bar{R} for all runs. It was found that most of these R_i were stable within the $\pm 3\sigma$ limits around the average values $\bar{R} \approx 1.05$, except for some runs and one of the periods.

Stability in the measurement of the hadron azimuthal angle ϕ is essential to be able to determine asymmetries. Distributions of ϕ -values were obtained for each run of data taking and average values $\langle \phi \rangle_i$ per run were determined. The distribution of $\langle \phi \rangle_i$ had a Gaussian shape and for most of runs their values were within the $\pm 3\sigma$ -limit around the mean value equal to zero for all runs.

3.4 Method of asymmetry calculation

Following Ref. [5], the acceptance-cancelling method was used to calculate the 2006 asymmetries. In order to cancel acceptances, this method utilises double ratios, i.e. the product of two ratios of events. For the three-cell target the method was modified as follows. The target cell M was artificially divided in two sub-cells $M1$ and $M2$, each 28 cm long, and two pairs of cells (U and $M1$) and ($M2$ and D) are considered below. The cells in each pair have equal lengths but opposite polarisations at a given solenoid field direction f . For each pair of cells at a given f , one can construct a double ratio using the number of SIDIS events or hadrons. These numbers, denoted as N_{pf}^i , were obtained from cell i with the cell polarisation sign p (+ or –). The number of events (hadrons) multiplied by an "acceptance factor" C_f^i (C_f^i is an inverse product of the beam intensity, target density and acceptance), $N_{pf}^i C_f^i$, is related to the corresponding cross section σ_+ or σ_- given below. At $f = +$, the two double ratios that can be

constructed for the $(U, M1)$ and for the $(M2, D)$ pairs are as follows:

$$\left[\frac{N_{++}^U C_+^U}{N_{-+}^{M1} C_+^{M1}} \right]_{G1} \cdot \left[\frac{N_{++}^{M1} C_+^{M1}}{N_{-+}^U C_+^U} \right]_{G2} = \left(\frac{\sigma_+}{\sigma_-} \right)_1^2, \quad \left[\frac{N_{++}^D C_+^D}{N_{-+}^{M2} C_+^{M2}} \right]_{G1} \cdot \left[\frac{N_{++}^{M2} C_+^{M2}}{N_{-+}^D C_+^D} \right]_{G2} = \left(\frac{\sigma_+}{\sigma_-} \right)_2^2. \quad (5)$$

In these expressions, the first (second) ratio is built using events or hadrons from G1 (G2) runs. If the acceptance factors are stable and equal during the G1 and G2 runs, they cancel in Eqs. (5). In the numerator of each ratio the events (hadrons) were taken from the runs with the positive target cell polarisation, while in the denominator they were taken from the runs with negative target polarisation. Thus each ratio in the left parts of Eqs. (5) is equal to the ratio of the total (or differential) SIDIS cross sections for the positive and negative target polarisations, σ_+/σ_- . Hence, two double ratios have to be equal within statistical uncertainties and expected to be close to unity. Similarly, at $f = -$, the two double ratios, which can be constructed for the $(U, M1)$ and $(M2, D)$ pairs, are as follows:

$$\left[\frac{N_{+-}^{M1} C_-^{M1}}{N_{--}^U C_-^U} \right]_{G1} \cdot \left[\frac{N_{+-}^U C_-^U}{N_{--}^{M1} C_-^{M1}} \right]_{G2} = \left(\frac{\sigma_+}{\sigma_-} \right)_3^2, \quad \left[\frac{N_{+-}^{M2} C_-^{M2}}{N_{--}^D C_-^D} \right]_{G1} \cdot \left[\frac{N_{+-}^D C_-^D}{N_{--}^{M2} C_-^{M2}} \right]_{G2} = \left(\frac{\sigma_+}{\sigma_-} \right)_4^2. \quad (6)$$

Thus each of four double ratios in Eqs. (5, 6) is related to the squared ratio of the SIDIS cross sections for positive and negative target polarisations determined with part of the full statistics. When statistically averaged, they can be used to calculate asymmetries (see Section 3.6) provided that: (i) acceptance factors in the G1 and G2 periods are indeed stable and equal and (ii) the values of the double ratios calculated for SIDIS events and for hadrons with polarisation settings at $f = +$ and $f = -$ are stable and equal within statistical uncertainties.

Altogether, the stability tests of acceptance factors and of the double ratios in Eqs. (5, 6) using SIDIS events and hadrons have shown that these ratios are mostly stable over the data taking periods and statistically well inside the $\pm 3\sigma$ corridors around the average values, which are close to unity.

3.5 Final selection of the 2006 SIDIS events and hadrons

In order to be accepted for analysis, for a given run the average value per run of the acceptance factors, the angles $\langle \phi \rangle_i$ and the double ratio values found with Eqs. (5, 6) had to be within $\pm 3\sigma$ limits of the corresponding mean value for all runs. Otherwise the run was rejected. The rejected runs contained about 10% of 2006 hadrons.

Distributions of selected SIDIS events or charged hadrons as a function of one of the kinematic variables Q^2 , y , z and p_T^h for different samples of data are presented in Fig. 2. As motivated in Ref. [5], the 2006 asymmetries were calculated in the regions of the kinematic variables x , Q^2 , z and p_T^h shown in Table 1.

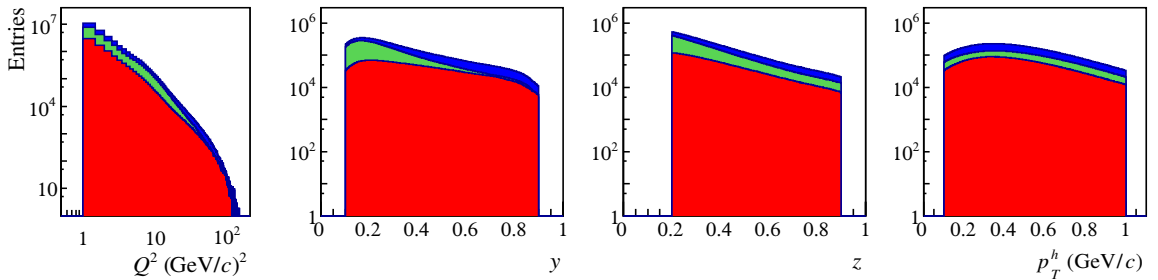


Fig. 2: Kinematic distributions of SIDIS events or charged hadrons within the selected cuts obtained from different samples of the data: 2006 (lower, red), 2002–2004 (middle, green) and 2002–2006 (upper, blue).

Table 1: Bin limits and their weighted mean values for the kinematic variables x , Q^2 , z and p_T^h .

x		Q^2 (GeV/c) ²		z		p_T^h (GeV/c)	
bin limits	mean	bin limits	mean	bin limits	mean	bin limits	mean
0.004 – 0.012,	0.010	1.0 – 3.0,	1.45	0.200 – 0.234,	0.216	0.100 – 0.239,	0.177
0.012 – 0.022,	0.020	1.0 – 6.0,	2.07	0.234 – 0.275,	0.253	0.239 – 0.337,	0.289
0.022 – 0.035,	0.031	1.0 – 9.5,	2.89	0.275 – 0.327,	0.299	0.337 – 0.433,	0.385
0.035 – 0.076,	0.053	1.0 – 20.0,	4.82	0.327 – 0.400,	0.361	0.433 – 0.542,	0.485
0.076 – 0.132,	0.098	2.0 – 35.0,	9.20	0.400 – 0.523,	0.455	0.542 – 0.689,	0.610
0.132 – 0.700,	0.190	3.0 – 100.0,	21.26	0.523 – 0.900,	0.661	0.689 – 1.000,	0.814

3.6 Calculation of azimuthal asymmetries in hadron production

For the calculation of the azimuthal asymmetries $a_{h^\pm}(\phi)$, the distributions of the charged hadrons h^+ and h^- were separately analysed as a function of the azimuthal angle ϕ and 10 ϕ -bins were used to cover the region $\pm 180^\circ$. For both h^+ and h^- , the double ratios defined in Eqs. (5, 6), $(\sigma_+/\sigma_-)_k^2(\phi)$, $k = 1, \dots, 4$, were calculated and combined as follows:

$$\left(\frac{\sigma_+}{\sigma_-}\right)_{h^\pm}^2(\phi) = \left[\left(\frac{\sigma_+}{\sigma_-}\right)_1^2 \oplus \left(\frac{\sigma_+}{\sigma_-}\right)_2^2 \oplus \left(\frac{\sigma_+}{\sigma_-}\right)_3^2 \oplus \left(\frac{\sigma_+}{\sigma_-}\right)_4^2 \right]_{h^\pm}(\phi) \cong 1 + a_{h^\pm}(\phi) \sum_k \left[\sum_{i,p \in k} \mathcal{P}_{pf}^i(x,y) \right]_{h^\pm} \cdot W_k, \quad (7)$$

where the symbol \oplus means statistically weighted averaging. As it was shown in Ref. [5], in first approximation the values of $(\sigma_+/\sigma_-)_{h^\pm}^2(\phi)$ are related to $a_{h^\pm}(\phi)$ multiplied by polarisation terms. For each hadron charge, the polarisation term is given by the sum of the $\mathcal{P}_{pf}^i(x,y)$ values, each of them being the product of target cell polarisations $|P_{pf}^i|$ and dilution factor (see Refs. [5, 11]), $f^i(x,y)$, where i , p and f are those used to calculate the ratio $(\sigma_+/\sigma_-)_k^2(\phi)$, i.e. four polarisation values at each k . The weight W_k is equal to the ratio of the number of hadrons, N_k , to the total number of hadrons, N_{tot} . Therefore, the asymmetries $a_{h^\pm}(\phi)$, referred to as single-hadron asymmetries, are given by expression:

$$a_{h^\pm}(\phi) \cong \frac{(\sigma_\pm/\sigma_\mp)_{h^\pm}^2(\phi) - 1}{\sum_k \left[\sum_{i,p \in k} \mathcal{P}_{pf}^i(x,y) \right]_{h^\pm} \cdot W_k}. \quad (8)$$

3.7 Asymmetries from the 2006 data

The 2006 asymmetries $a_{h^\pm}(\phi)$ were calculated both (i) integrating the hadron distributions over the COMPASS region of the kinematic variables x , p_T^h and z (integrated asymmetries) and (ii) as a function of one of these variables disregarding the other two. In each case, the asymmetries were fitted by the function from Eq. (4) using the standard least square method and extracting all asymmetry modulation amplitudes at once. The results of fitting the 2006 integrated asymmetries together with those of the 2002–2004 [5] are shown in Fig. 3. The modulation amplitudes obtained for each year are in agreement with one another. The values of the modulation amplitudes combined from the fits of the 2002–2004 and 2006 data, denoted by AV, are also shown in Fig. 3.

The 2006 modulation amplitudes as a function of kinematic variables were compared to those from the combined 2002–2004 data and also found to be in agreement within statistical uncertainties.

In order to check the impact of the disregarded modulations, which could have appeared from SIDIS partial cross sections $d\sigma_{00}$ and $d\sigma_{L0}$, on the modulation amplitudes in Eq. (4), we have performed fits of the 2006 asymmetries by a new fitting function which contains a numerator and denominator. In the numerator we have used the same modulations as in Eq. (4), but in the denominator we included the disregarded modulation with average amplitudes determined in Ref. [2]. For the asymmetry $a_{h^-}(\phi)$ it is

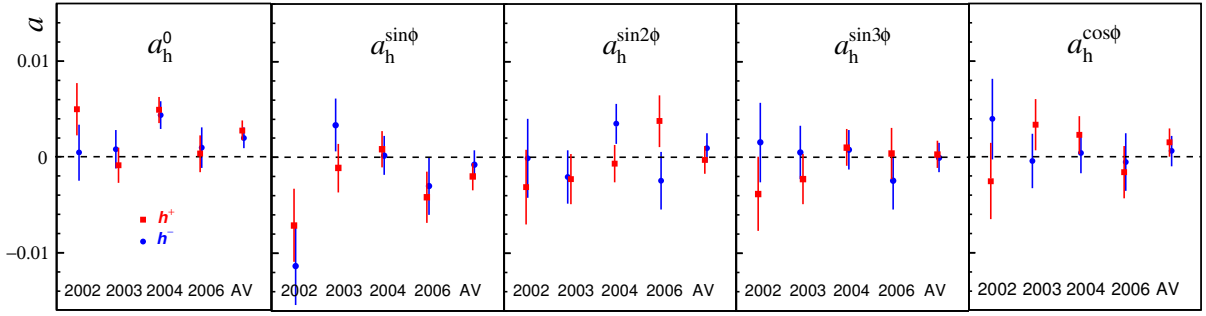


Fig. 3: The values of modulation amplitudes a obtained from the fits of the integrated asymmetries $a_{h^\pm}(\phi)$ by the function from Eq. (4) separately for the data of 2002, 2003, 2004 and 2006 as well as for combined data of 2002–2006 (AV). Only statistical uncertainties are shown.

as follows:

$$a_{h^-}(\phi) = \frac{a_{h^-}^0 + a_{h^-}^{\sin\phi} \sin\phi + a_{h^-}^{\sin 2\phi} \sin 2\phi + a_{h^-}^{\sin 3\phi} \sin 3\phi + a_{h^-}^{\cos\phi} \cos\phi}{1 + 0.0412 \cos 2\phi + 0.0552 \cos\phi + 0.0008 \sin\phi}. \quad (9)$$

Comparing results of this fit with results of the standard fit of the 2006 data shown in Fig. 3, it was found that the differences between values of modulation amplitudes in the numerator are smaller than 0.01 of the statistical uncertainties. Similar results are obtained for $a_{h^+}(\phi)$ replacing amplitudes in the denominator of Eq. (9) by corresponding values from Ref. [2]. Thus the contributions to the asymmetries in Eq. (4), which could have appeared from the denominator of Eq. (3), are indeed negligible.

4 Azimuthal asymmetries for combined deuteron data

4.1 Integrated asymmetries

The values of the modulation amplitudes that were obtained for the combined 2002–2006 data on the integrated asymmetries (AV) are given in Table 2. As expected, consistent results are obtained for the ϕ -independent terms $a_{h^+}^0$ and $a_{h^-}^0$. All other modulation amplitudes are consistent with zero within statistical uncertainties.

Table 2: The modulation amplitudes of the h^+ and h^- integrated azimuthal asymmetries obtained from the combined data on the muon SIDIS off longitudinally polarised deuterons. Only statistical uncertainties are shown.

Modulation amplitudes	Amplitudes in 10^{-3} units	
	h^+	h^-
a^0	2.81 ± 0.96	2.01 ± 0.98
$a^{\sin\phi}$	-1.93 ± 1.31	-0.74 ± 1.41
$a^{\sin 2\phi}$	-0.29 ± 1.33	-0.74 ± 1.41
$a^{\sin 3\phi}$	0.34 ± 1.36	-0.10 ± 1.42
$a^{\cos\phi}$	1.52 ± 1.32	0.66 ± 1.42

4.2 Asymmetries as functions of kinematic variables

The final 2002–2006 results on the modulation amplitudes of asymmetries $a_{h^\pm}(\phi)$ calculated as a function of one of the variables x , z and p_T^h while disregarding the other two are presented in Fig. 4.

Except for the amplitudes $a_{h^\pm}^0(x)$, all other amplitudes, when fitted by constant, are found to be consistent with zero within statistical uncertainties. The amplitudes $a_{h^\pm}^0(x)$ have the same x -dependences for positive and negative hadrons. Additionally, the x -dependences of the $a_{h^\pm}^0(x)/D_0(x,y)$ values are presented

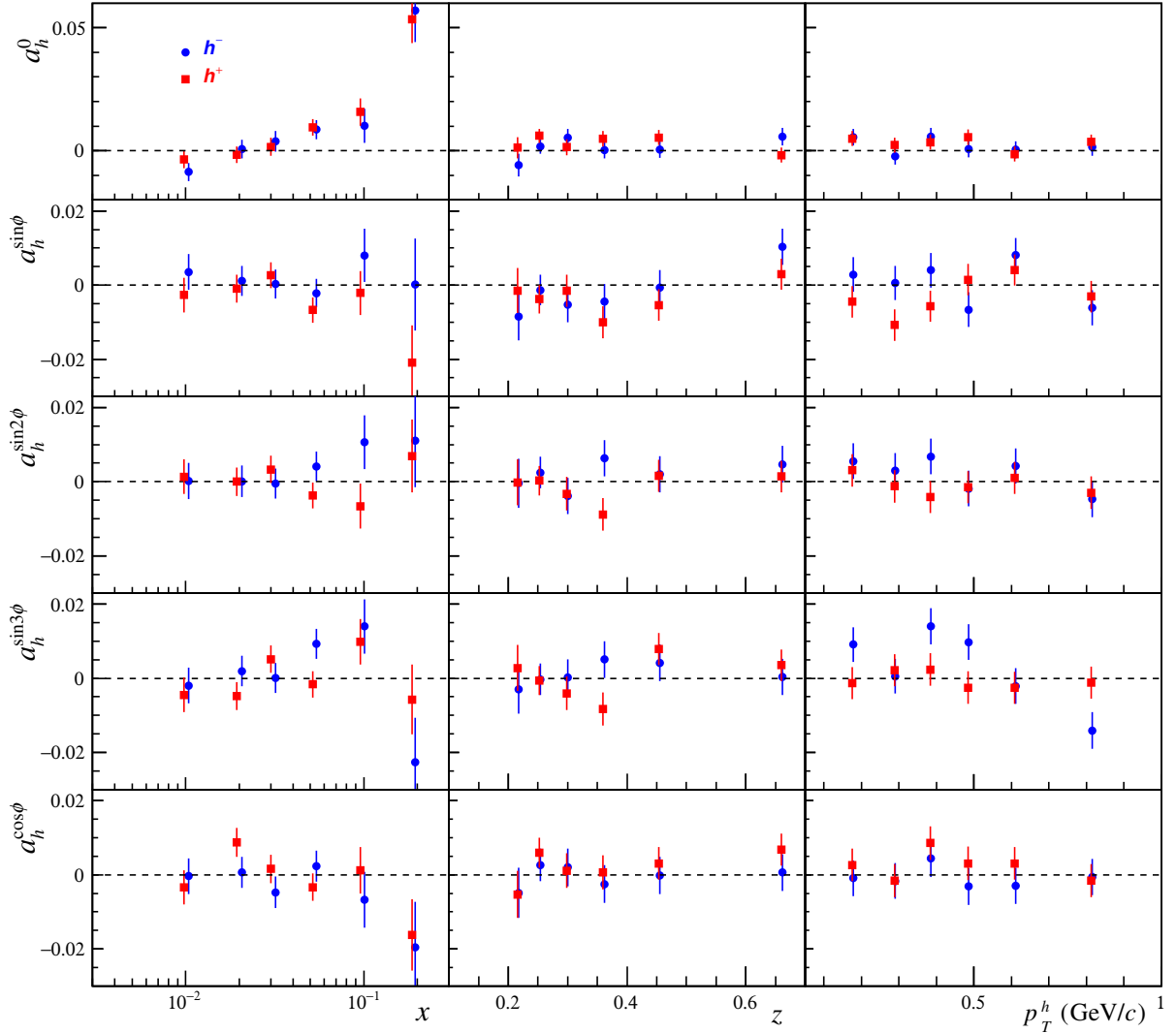


Fig. 4: The modulation amplitudes of the h^+ and h^- azimuthal asymmetries as a function of x , z and p_T^h obtained from the combined 2002–2006 data on the muon SIDIS off longitudinally polarised deuterons. Only statistical uncertainties are shown.

in Fig. 5, where $D_0(x, y)$ is the virtual-photon depolarisation factor multiplied by the average beam polarisation $|P_\mu|$ as defined in Ref. [5] for each x -bin. If the amplitudes $a_{h^\pm}^0(x)$ represent main contributions to the asymmetries of Eq. (3), the values of $a_{h^\pm}^0(x)/D_0(x, y)$ by definition (see e.g. Ref. [12]) are equal to the asymmetries $A_{1d}^{h^\pm}(x)$. Within experimental uncertainties, there is good agreement between our data on $a_{h^\pm}^0(x)/D_0(x, y)$ and the data of Ref. [13] on $A_{1d}^{h^\pm}(x)$, which confirms the correctness of the results on the asymmetries calculated by the modified acceptance-cancelling method. The values of $A_{1d}^{h^\pm}(x)$ were obtained with the 2002–2004 data. A similar x -dependence was also observed with 2002–2006 data for the asymmetries $A_{1d}^{\pi^\pm}(x)$ and $A_{1d}^{K^+}(x)$ obtained with identified pions and positive kaons, respectively Ref. [6].

5 Systematic uncertainties

The compatibility of the results on the asymmetries $a_{h^\pm}(\phi)$ that were obtained separately for 2002, 2003, 2004 and 2006 years was checked by building the pull distributions: $pulls_i = (a_i - \langle a \rangle) \cdot |\sigma_{a_i}^2 - \sigma_{\langle a \rangle}^2|^{-1/2}$, where a_i is the asymmetry for a given year, hadron charge and kinematic bin, $\langle a \rangle$ is the corresponding weighted mean value over four years and σ denotes the corresponding standard deviation. The distri-

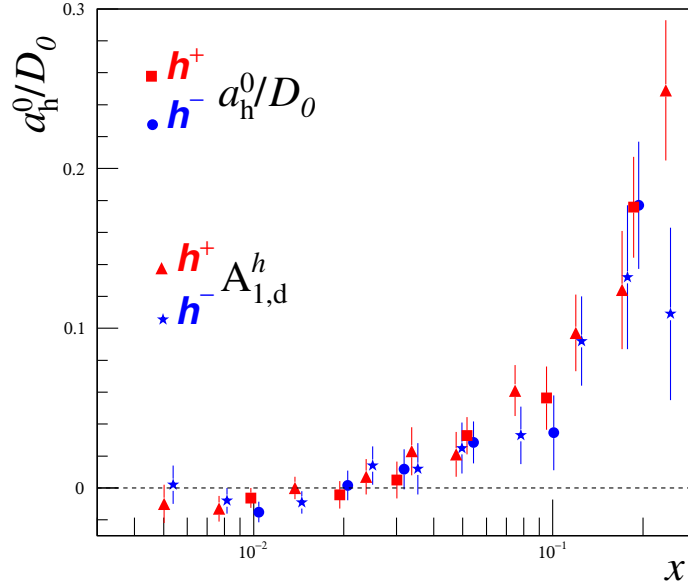


Fig. 5: The x -dependences of the $a_{h^\pm}^0(x)/D_0(x,y)$ values for 2002–2006 data in comparison with the data of Ref. [13] on $A_{1,d}^{h^\pm}(x)$.

bution had 750 entries in total. As expected, it follows a Gaussian distribution with the mean value consistent with zero and σ with unity. This indicates that no significant systematic effects were present in the data on asymmetries.

The stability of hadron yields in the 2006 data was checked following the procedure described in Ref. [5]. For this purpose, the double ratios of hadron numbers as a function of the azimuthal angle ϕ for different polarisation settings at the field f were calculated as follows:

$$f = + : F_+(\phi) = \frac{N_{++}^U + N_{++}^D}{N_{-+}^M} \cdot \frac{N_{++}^M}{N_{-+}^U + N_{-+}^D}, \quad f = - : F_-(\phi) = \frac{N_{+-}^U + N_{+-}^D}{N_{--}^M} \cdot \frac{N_{+-}^M}{N_{--}^U + N_{--}^D}. \quad (10)$$

Here, N_{pf}^i is the number of hadrons from target cell i with polarisation p and field f , as explained in Section 3.4. These ratios are independent of acceptance and muon flux. They are modifications of similar ratios used in Ref. [5] for the case of two target cells. The fits by constants of the weighted sums $F(\phi) = F_+(\phi) \oplus F_-(\phi)$ for h^+ , h^- and $h^+ + h^-$ of the 2006 data gave results consistent with unity within statistical uncertainties of the order of 0.001. This means that no acceptance-changing effects have been observed, i.e. there are no large additive systematic uncertainties in the 2006 data.

Possible sources of systematic uncertainties in the asymmetry evaluation are uncertainties in the determination of the beam and target polarisations, the estimation of the dilution factor and a possible variation of acceptance. Since the compatibility and stability tests have not revealed any significant systematic effects due to acceptance variations, these effects are considered to be smaller than the statistical uncertainties. As a quantitative measure of possible additive systematic uncertainties in the 2006 asymmetry measurements, the value $\Delta a_{h^\pm}(\phi) = \pm 0.003$ was chosen, which is equal to $\pm 3\sigma$ of the $h^+ + h^-$ data stability test for $F(\phi)$. The same value was also obtained for the 2002–2004 data Ref. [5] and hence adopted also for the combined deuteron data. The multiplicative systematic uncertainties of the extracted asymmetries due to uncertainties in the determination of the beam and target polarisations were estimated to be less than 5% each and those due to uncertainties of the dilution factor to be less than about 2%. When combined in quadrature, an overall multiplicative systematic uncertainty of less than 6% was obtained.

6 Conclusions

The searches for possible azimuthal modulations in the single-hadron azimuthal asymmetries $a_{h^\pm}(\phi)$, as manifestation of TMD PDFs describing the nucleons in longitudinally polarised deuteron, have been performed using all COMPASS deuteron data and the acceptance-cancelling method of analysis. For each hadron charge, beside the ϕ -independent term, four possible modulations predicted by theory ($\sin\phi$, $\sin 2\phi$, $\sin 3\phi$ and $\cos\phi$) and their dependence on kinematical variables are considered.

The ϕ -independent terms $a_{h^\pm}^0(x)$ of the asymmetries $a_{h^\pm}(\phi)$, which are expected to originate mostly from the known helicity PDFs $g_{1L}(x) \equiv g_1(x)$, are connected to the virtual photon asymmetry $A_{1d}^{h^\pm}(x) = a_{h^\pm}^0(x)/D_0(x,y)$. There is good agreement between the COMPASS data on $a_{h^\pm}^0(x)/D_0(x,y)$ and $A_{1d}^{h^\pm}(x)$ from Refs. [6, 13], which confirms this expectation.

No statistically significant dependence of other ϕ -modulation amplitudes was observed in the variables x , z or p_T^h . Still, there are indications for a possible x -dependence of the $\sin 2\phi$ and $\cos\phi$ amplitudes. The $\sin 2\phi$ amplitude for h^- is mostly positive and rises with increasing x , while for h^+ it is mostly negative and decreases with x . This behaviour agrees with that discussed in Refs. [7, 14] if one takes into account different sign convention used for determination of asymmetries by HERMES and COMPASS collaborations. The increase with x of the modulus of the $\cos\phi$ amplitudes, related to the Cahn-effect [15] and predicted in Ref. [16], was already visible from the 2002–2004 data [5] and persists for the combined 2002–2006 data. Quantitative estimates of a possible contribution of the $\cos\phi$ modulation to the deuteron asymmetries, related to twist-3 TMD PDFs g_L^\perp and e_L , have been obtained in Ref. [17]. They are in agreement with our data.

Altogether, one can conclude that TMD PDFs contributions to the azimuthal asymmetries in the cross sections of hadron production in muon SIDIS off longitudinally polarised deuterons are small. This is either due to possible cancellations of the contributions to the asymmetries by the deuteron up and down quarks, or/and due to the smallness of the transverse component of the target polarisation and of the suppression factor that behaves as M/Q . Some of these conclusions can be checked studying these asymmetries in muon SIDIS off longitudinally polarised protons.

Acknowledgements

We gratefully acknowledge the support of our funding agencies and of the CERN management and staff and the skills and efforts of the technicians of our collaborating institutes. Special thanks go to V. Anosov and V. Pesaro for their technical support during the installation and running of this experiment.

References

- [1] A. Bacchetta, M. Diehl, K. Goeke, A. Metz, P. J. Mulders and M. Schlegel, *JHEP* **0702** (2007) 093 [arXiv:hep-ph/0611265].
- [2] C. Adolph *et al.* [COMPASS Collaboration], *Nucl. Phys. B* **886** (2014) 1046 [arXiv:1401.6284].
- [3] C. Adolph *et al.* [COMPASS Collaboration], *Phys. Lett. B* **717** (2012) 383 [arXiv:1205.5122].
C. Adolph *et al.* [COMPASS Collaboration], *Phys. Lett. B* **717** (2012) 376 [arXiv:1205.5121].
C. Adolph *et al.* [COMPASS Collaboration], *Phys. Lett. B* **736** (2014) 124 [arXiv:1401.7873].
- [4] C. Adolph *et al.* [COMPASS Collaboration], *Phys. Lett. B* **744** (2015) 250 [arXiv:1408.4405].
- [5] M. G. Alekseev *et al.* [COMPASS Collaboration], *Eur. Phys. J. C* **70** (2010) 39 [arXiv:1007.1562].
- [6] M. Alekseev *et al.* [COMPASS Collaboration], *Phys. Lett. B* **680** (2009) 217 [arXiv:0905.2828].
- [7] A. Airapetian *et al.* [HERMES Collaboration], *Phys. Lett. B* **562** (2003) 182 [arXiv:hep-ex/0212039].
- [8] M. Arneodo *et al.* (European Muon Collaboration), *Z. Phys. C* **34** (1987) 277.

-
- [9] A. Airapetian *et al.* [HERMES Collaboration], Phys. Rev. D **87** (2013) 012010 [arXiv:1204.4161 [hep-ex]].
- [10] P. Abbon *et al.* [COMPASS Collaboration], Nucl. Instrum. Meth. A **577** (2007) 455 [hep-ex/0703049].
- [11] E. S. Ageev *et al.* [COMPASS Collaboration], Phys. Lett. B **612** (2005) 154 [hep-ex/0501073].
- [12] M. Anselmino, A. Efremov and E. Leader, Phys. Rept. **261** (1995) 1; Erratum: [Phys. Rept. **281** (1997) 399] [hep-ph/9501369].
- [13] M. Alekseev *et al.* [COMPASS Collaboration], Phys. Lett. B **660** (2008) 458 [arXiv:0707.4077].
- [14] H. Avakian, A. V. Efremov, K. Goetze, A. Metz, P. Schweitzer and T. Teckentrup, Phys. Rev. D **77** (2008) 014023 [arXiv:0709.3253].
- [15] R. N. Cahn, Phys. Lett. B **78** (1978) 269; Phys. Rev. D **40** (1989) 3107.
- [16] M. Anselmino, A. Efremov, A. Kotzinian and B. Parsamyan, Phys. Rev. D **74** (2006) 074015 [hep-ph/0608048].
- [17] W. Mao, X. Wang, X. Du, Z. Lu and B.Q. Ma, Nucl. Phys. A **945** (2016) 153.